Initiation Mechanisms and Kinetics of Pyrolysis and Combustion of JP-10 Hydrocarbon Jet Fuel

Kimberly Chenoweth,[†] Adri C. T. van Duin,[‡] Siddharth Dasgupta, and William A. Goddard III*

Materials and Process Simulation Center (139-74), California Institute of Technology, Pasadena, California 91125

Received: September 12, 2008; Revised Manuscript Received: December 01, 2008

In order to investigate the initiation mechanisms and kinetics associated with the pyrolysis of JP-10 (*exo*-tricyclo[5.2.1.$0^{2,6}$]decane), a single-component hydrocarbon jet fuel, we carried out molecular dynamics (MD) simulations employing the ReaxFF reactive force field. We found that the primary decomposition reactions involve either (1) dissociation of ethylene from JP-10, resulting in the formation of a C_8 hydrocarbon intermediate, or (2) the production of two C_5 hydrocarbons. ReaxFF MD leads to good agreement with experiment for the product distribution as a function of temperature. On the basis of the rate of consumption of JP-10, we calculate an activation energy of 58.4 kcal/mol for the thermal decomposition of this material, which is consistent with a strain-facilitated C−C bond cleavage mechanism in JP-10. This compares well with the experimental value of 62.4 kcal/mol. In addition, we carried out ReaxFF MD studies of the reactive events responsible for oxidation of JP-10. Here we found overall agreement between the thermodynamic energies obtained from ReaxFF and quantum-mechanical calculations, illustrating the usefulness of ReaxFF for studying oxidation of hydrocarbons. The agreement of these results with available experimental observations demonstrates that ReaxFF can provide useful insights into the complicated thermal decomposition and oxidation processes of important hydrocarbon fuels.

Introduction

JP-10 (*exo*-tricyclo[5.2.1.$0^{2,6}$]decane, Figure 1) is a single-component fuel being studied for use in pulse-detonation engines (PDEs), where operational conditions involve high temperatures (1000−2500 K) and high pressures (1−100 bar).[1] PDEs operate through filling of a cylinder with fuel followed by detonation of the fuel in the combustion chamber. This produces a shock wave that propagates down the cylinder, compressing the remaining fuel, which ignites and generates a pulse of thrust. PDEs have the potential to produce a higher burn and thermodynamic efficiency because the combustion occurs as detonation rather than deflagration. Consequently, they are being investigated for lightweight, low-cost, fuel-efficient space propulsion systems and for other flight systems. The hydrocarbon jet fuel JP-10 is being targeted for use in PDEs because of its high thermal stability, high energy density, low cost, and widespread availability.[2] JP-10 is synthetically prepared from the hydrogenation of dicyclopentadiene, and there is 23.8 kcal/mol of strain energy resulting from the tricyclic geometry of JP-10.[4,5]

While good information about the thermochemical and thermophysical properties of JP-10 is available,[6] less is known regarding the detailed mechanisms of pyrolysis and combustion of this material. In addition, existing JP-10 kinetic models are inconsistent with experimental results.[7,8] Thermal decomposition, catalytic cracking, and shock tube studies have provided insight into the overall chemistry of JP-10 decomposition, but the details of the initiation reactions and the high-temperature chemistry are still not well-established.[1,4,5,7−14] The products observed experimentally from the thermal decomposition of JP-10 are summarized from the literature in Table 1. The pyrolysis products common to all of the experiments are benzene and cyclopentadiene (CPD), but there is no agreement on whether the formation of these products results from primary or secondary chemistry. It has been observed that either the formation of CPD decreases at high temperatures or the CPD decomposes to a variety of C_2, C_3, and C_4 species.[5,8] The variation in experimental conditions and methods of analysis might explain the diversity of the observed products.

To gain insight into the initiation mechanism for JP-10 pyrolysis and combustion, we performed molecular dynamics

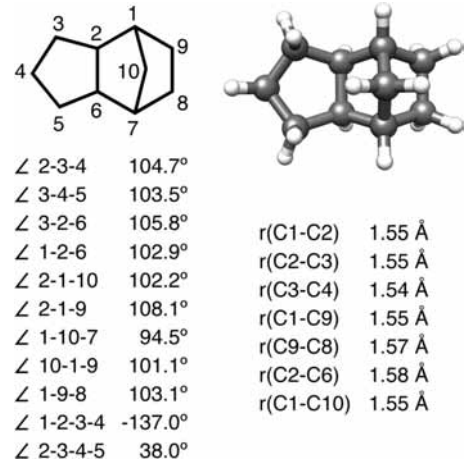

Figure 1. Structure of JP-10.

* To whom correspondence should be addressed. E-mail: wag@wag.caltech.edu
† Present address: Department of Chemistry, Smith College, Northampton, MA 01063.
‡ Present address: Department of Mechanical and Nuclear Engineering, The Pennsylvania State University, University Park, PA 16802.

10.1021/jp8081479 CCC: $40.75
Published on Web 02/11/2009

TABLE 1: Summary of JP-10 Decomposition Products (All Results Are from Experiment except Those in the ReaxFF Column)

decomposition products	ref 4[a]	ref 5[b]	ref 7[c]	ref 8[d]	ref 11[e]	ref 12[f]	ReaxFF[g]
H_2			√			√	√
CH_4			√			√	√
C_2H_2	√	√		√		√	√
C_2H_4	√	√	√	√		√	√
C_2H_6			√			√	√
C_3H_4 (propyne)		√		√			√
C_3H_5 (allyl radical)							√
C_3H_6 (propene)	√		√			√	√
C_3H_8 (propane)						√	
C_4H_6 (1,3-butadiene)	√					√	√
C_4H_8 (1-butene)						√	√
C_4H_8 (2-butene)						√	
C_4H_8 (isobutylene)						√	
C_4H_{10} (n-butane)							
C_4H_x		√		√ ($x = 4, 6, 8$)			√ ($x = 5$)
C_5H_6 (cyclopentadiene)	√	√	√	√	√	√	
C_5H_8 (cyclopentene)	√		√		√	√	√
C_5H_8 (1,4-pentadiene)							√
C_5H_x	√ ($x = 6, 8$)						√ ($x = 6, 7$)
C_6H_6 (benzene)	√	√	√	√	√	√	
C_6H_{10} (1,5-hexadiene)			√				√
C_6H_x				√			√ ($x = 8, 9$)
C_7H_9 (toluene)			√		√	√	
C_7H_x		√		√ ($x = 6, 8, 10$)			√ ($x = 10, 11$)
C_8H_x				√			√ ($x = 10, 12$)
C_9H_x							√ ($x = 14$)
$C_{10}H_8$ (napthalene)					√	√	
$C_{10}H_{12}$ (dicyclopentadiene)						√	
$C_{10}H_{16}$ (cyclopentylcyclopentene)			√				√
$C_{10}H_x$				√			√ ($x = 15, 17$)
C_nH_x ($n > 10$)							√

[a] $T = 1100-1700$ K; 250 ppm JP-10 in argon. [b] $T = 300-1400$ K; 3.9% JP-10 in helium. [c] $T = 848-933$ K; 96.6 wt % exo form; 2.5 wt % endo form; 0.7−4% JP-10 in helium. [d] $T = 300-1700$ K; 5% JP-10 in argon or helium. [e] $T = 473-923$ K; no inert gases added to the JP-10 feed. [f] $T = 903-968$ K; no inert gases added to the JP-10 feed. [g] $T = 2000-2600$ K; product list obtained from ReaxFF NVT-MD simulations of JP-10.

(MD) simulations employing the ReaxFF reactive force field,[15] which has been used to study complicated decomposition processes in various materials including RDX,[16] TATP,[17] and PDMS polymer.[18] Recently, the ReaxFF force field was expanded to improve the description of hydrocarbon oxidation,[19] and it provided useful insight into the initial reactive events for oxidation of various hydrocarbons (i.e., methane, propene, *o*-xylene, and benzene) under extreme conditions. Here, we employed the updated ReaxFF force field for hydrocarbons to study the initiation reactions and kinetics associated with pyrolysis and combustion of JP-10. We present results from a series of NVT-MD simulations that provide not only the initial reactive events but also the overall product distributions as a function of temperature. In addition, we measured the rate of JP-10 decomposition and calculated the activation energy for the process. Finally, we present results from an initial NVT-MD simulation of JP-10 oxidation. We also compare them to the results of quantum-mechanical (QM) calculations and experiment in order to validate the predictions made by the ReaxFF force field.

Computational Approach

The full set of ReaxFF parameters used in these studies is collected in the Supporting Information along with a full description of the ReaxFF potential functions.

MD Simulations were performed on pure JP-10 and on JP-10 exposed to oxygen radicals. In order to study the pyrolysis of JP-10, we placed 40 JP-10 molecules in a unit cell measuring 36 Å × 36 Å × 18 Å. The system was minimized using low-temperature (5 K) MD and then equilibrated with NVT-MD for 10 ps at 1500 K using a time step of 0.1 fs. All of the MD simulations were performed with a constant number of atoms (N) in a constant volume (V) with control of the temperature (T) using a thermostat; we designate these conditions as NVT. The temperature was controlled with Berendsen thermostat[20] using a 0.2 ps damping constant. The equilibrated system had a density of 0.39 g/cm^3 and a pressure of approximately 106 MPa = 0.106 GPa = 1060 bar, which can easily occur in many reactive processes, including rocket engines and shock-induced reactions, but may be a bit high for typical combustion or pyrolysis experiments.

After equilibration, 10 unique starting configurations were collected and used for a series of NVT-MD simulations at temperatures of 2000, 2100, 2200, 2300, 2400, 2500, and 2600 K for a total simulation time of 50 ps. The results from these 10 simulations were averaged to investigate the kinetics of decomposition, and the overall product distributions varied as a function of the different temperatures studied.

In addition to studying the pyrolysis processes, we also carried out MD simulations to study the initiation mechanisms for JP-10 combustion. The system was composed of five JP-10 molecules exposed to 10 oxygen radicals. The system was first minimized using low-temperature MD (10 K) and then equilibrated at 1000 K for 5 ps using a temperature damping constant of 0.1 ps and a time step of 0.25 fs. During the equilibration simulation, the C−O and H−O attractive bond terms were switched off to prevent reactions from occurring. The equilibrated system had a density of 0.17 g/cm^3 and a pressure of 36

MPa. The equilibrated system was then used in a 10 ps NVT-MD simulation at 1000 K with a temperature damping constant of 0.1 ps and a time step of 0.25 fs.

We analyzed the intermediates and products formed during the MD simulation using a 0.2 bond-order cutoff for molecular recognition. We use this low cutoff for molecular identification in these low-density simulations in order to capture all of the reactive processes, including unsuccessful events that produce very short-lived species. The choice of bond-order cutoff does not affect the simulation itself but only affects its interpretation in terms of chemical components.

Validation of the force field was carried by performing QM calculations on selected intermediates using the B3LYP[21] hybrid DFT functional and the Pople 6-311G** basis set[22] as implemented in Jaguar (version 7.0).[23] These results are presented below.

Results and Discussion

NVT-MD simulations were performed on a periodic cell containing 40 JP-10 molecules at high temperatures to investigate the both the initiation reactions and the kinetics of the pyrolysis processes, including the effects of temperature on the product distribution. Detailed analyses were carried out for the simulations at 2000 and 2200 K, leading to the results for product formation as a function of simulation time presented in Figure 2.

At 2000 K (Figure 2a), the initial steps convert JP-10 molecules to 1,4-pentadiene and cyclopentene at 18.1 and 24.8 ps. The unimolecular decomposition of JP-10 proceeds in less than 0.8 ps of simulation time through a stepwise mechanism involving sequential cleavage of C−C bonds between carbons 8 and 9, then carbons 1 and 2, and finally carbons 6 and 7 (for the atom-labeling scheme, see Figure 1), resulting in cyclopentene and 1,4-pentadiene. Indeed cyclopentene has been observed experimentally,[7,8,11,12] and Rao and Kunzru[12] and Davidson et al.[4] determined cyclopentene to be an initial decomposition product in their experiments. We find that two additional JP-10s decompose to form ethylene and 1,5-cyclooctadiene at 34.7 and 49.5 ps. This decomposition results from the formation of a biradical at carbons 2 and 6 followed by dissociation of C_2H_4 in a stepwise mechanism. While the concerted retro-Diels−Alder mechanism is possible, we only observe intermediates along a stepwise retro-decomposition pathway. This production of ethylene is consistent with experimental observations,[4,5,7,8,12] but there is no experimental evidence for a cyclooctadiene intermediate, which could be attributed to its reactivity under pyrolysis conditions. Indeed, this is consistent with ReaxFF simulations at higher temperatures, where we find that cyclooctadiene undergoes ring opening and further decomposition in <1 ps.

The NVT-MD simulation at 2200 K (Figure 2b) shows an increase in the number and diversity of the products from JP-10 decomposition, with primary decomposition products including C_2H_4, C_5H_8, and C_8H_{12} following the same initial reactive events observed at 2000 K (Figure 3). After 30 ps, we observe formation of allyl radicals from secondary reactions, which may be the precursor to propene or propyne via reactions with other intermediates to add or remove a hydrogen. Both propene[4,7,12] and propyne[5,8] have been observed experimentally. We find rapid decomposition (0.3 ps) of the unstable C_8 diradical (Figure 3) at 49.5 ps to form two 1,3-butadiene (C_4H_6) molecules. 1,3-Butadiene has also been observed experimentally by Davidson et al.[4] and Rao and Kunzru.[12] The remaining intermediates formed from secondary reactions during the 2200 K simulation (grouped together as "Others" in Figure 2b) include 1,3,9,13-tetradecatetraene ($C_{14}H_{22}$) and the 1,4-pentadiene radical (C_5H_7).

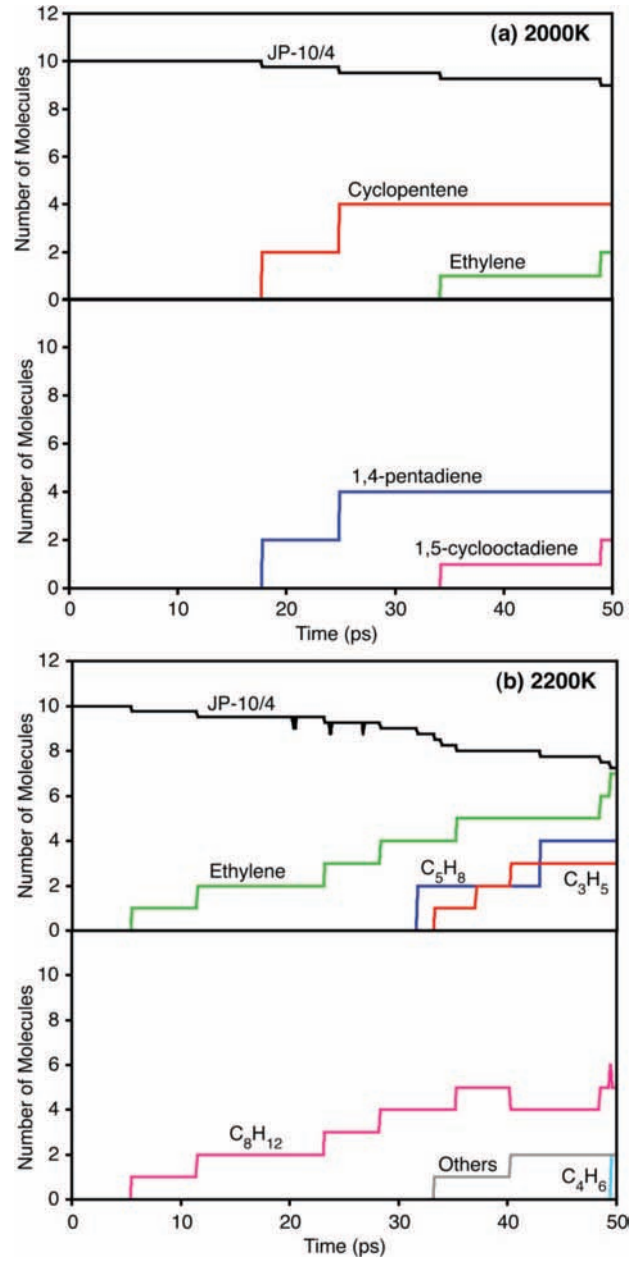

Figure 2. Decomposition products from ReaxFF MD as a function of simulation time at (a) 2000 and (b) 2200 K. The number of JP-10 molecules has been divided by 4, and only major products are shown explicitly; all of the intermediates and minor products are included together as "Others".

Initial reactive events predicted from the ReaxFF NVT-MD simulations were validated by performing QM calculations on molecules taken directly from ReaxFF trajectories. The structures were optimized using both QM and ReaxFF to obtain reaction energies at 0 K, which are given in Figure 3. Some reactions were observed to occur multiple times, and each of these is labeled with a number indicating how many JP-10 molecules (out of 40) were consumed by that particular reaction. The thermodynamic comparisons in Figure 3 reveal that ReaxFF provides a reasonable description of the energetics associated with these reactions. This agreement provides validation for the use of the ReaxFF method to investigate the pyrolysis of JP-10.

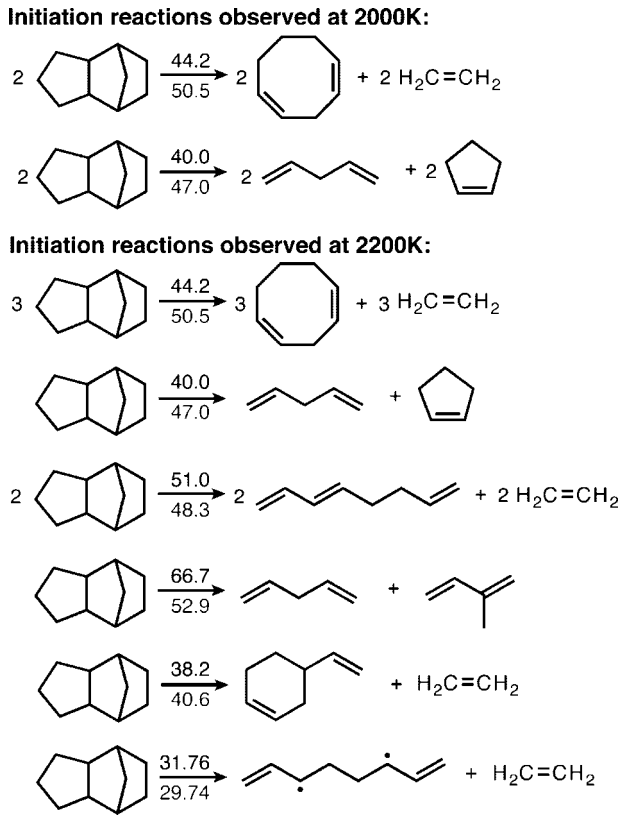

Figure 3. Reaction energies (kcal/mol) at 0 K for initiation reactions observed during ReaxFF NVT-MD simulations of JP-10 at 2000 and 2200 K, obtained using QM (black, above the arrows) and ReaxFF (gray, below the arrows). Reactions that occurred multiple times are indicated with the appropriate number (e.g., for the top reaction, the 2's indicate that two JP-10 molecules out of the 40 decomposed to form two 1,5-cyclooctadiene and two ethene molecules).

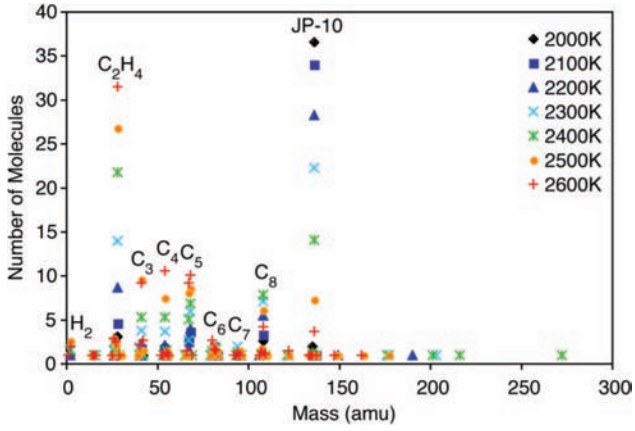

Figure 4. Superposition of final product distributions (depicted as mass spectra) at $t = 50$ ps from the average final configurations obtained at various temperatures using ReaxFF NVT-MD simulations. Every average final configuration was obtained from 10 independent simulations.

Detailed analysis of the mechanisms observed during the decomposition of JP-10 at 2000 and 2200 K indicates that the primary initiation pathways involve formation of ethylene and C_5 hydrocarbons. To gain insight into how the product distribution varies as a function of temperature, we carried out a series of 10 NVT-MD simulations at temperatures ranging from 2000 to 2600 K. The product distributions obtained from the final system configuration were averaged for each temperature, and

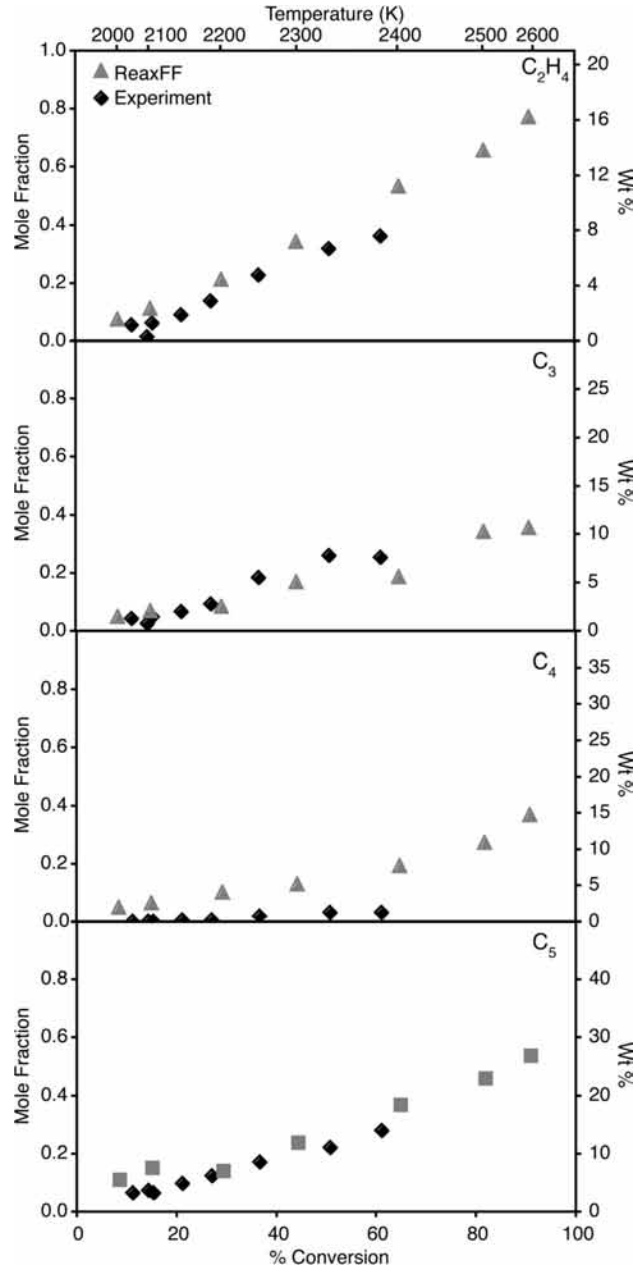

Figure 5. Average product distribution of C_2H_4 and C_3, C_4, and C_5 species obtained from (gray ▲ and ■) ReaxFF simulations at $t = 50$ ps (averaged over 10 independent simulations) and (black ◆) experiments by Rao and Kunzru performed over the temperature range 903−968 K.[12] The temperature of the ReaxFF NVT-MD simulation corresponding to each level of conversion is shown on the secondary x axis.

the resulting distribution of molecular weights is provided in Figure 4. Our results show that as the temperature increases from 2000 to 2600 K, the amount of unreacted JP-10 decreases while the quantities of C_2, C_3, C_4, and C_5 hydrocarbons increase. This is consistent with mass spectra measured during the pyrolytic breakdown of JP-10, which indicate a shift to lower-molecular-weight species on going from 920 to 1230 K.[8] It is interesting to note that the quantity of C_8 species reaches a maximum at 2400 K (Figure 4), indicating the instability of these species at high temperatures. In addition, we observe the formation of a small amount of H_2, which, although experimentally difficult to measure, has been observed experimentally by Rao and Kunzru[12] and Herbinet et al.[7]

Figure 5 shows the mole fractions of C_2H_4 and C_3, C_4, and C_5 products as functions of the percent conversion of JP-10

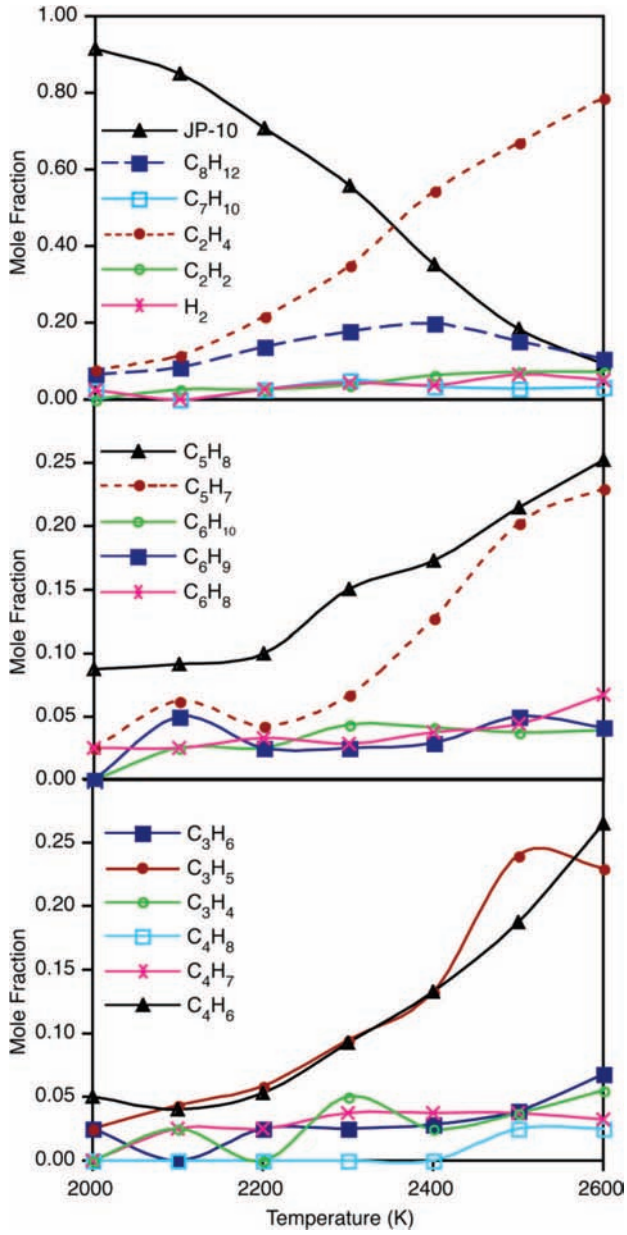

Figure 6. Average variation in product distribution as a function of temperature, as observed from ReaxFF NVT-MD simulations at t = 50 ps. The results were obtained from 10 independent simulations at each temperature.

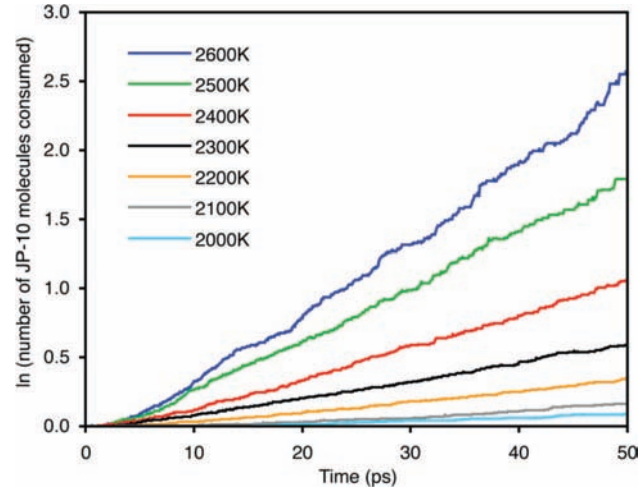

Figure 7. Average rates of JP-10 consumption observed during ReaxFF NVT-MD simulations at various temperatures. The results were obtained from 10 independent simulations at each temperature.

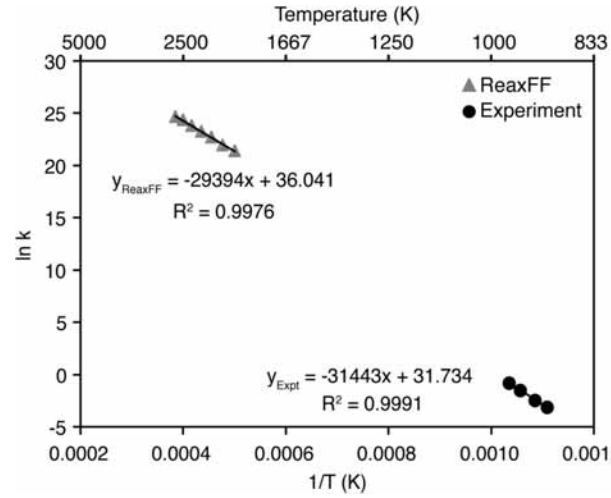

Figure 8. Arrhenius plot for the thermal decomposition of JP-10. The ReaxFF results are from Figure 7 and lead to $k = A \exp(-E_a/RT)$ with $A = 0.45 \times 10^{14}$ s^{-1} and E_a = 58.4 kcal/mol. The experimental data were obtained from Rao and Kunzru[12] and lead to $A = 57 \times 10^{14}$ s^{-1} and E_a = 62.4 kcal/mol.

(obtained by averaging the amounts of conversion obtained at each temperature). The trend obtained from ReaxFF is in good agreement with the experimental results from the pyrolysis studies performed by Rao and Kunzru[12] (Table 1). The types and mole fractions of the hydrocarbon intermediates observed during the thermal decomposition of JP-10 are shown in Figure 6, where the most abundant product at all temperatures is ethylene. In addition, we find that the formation of C_8H_{12} reaches a maximum at 2400 K, which is consistent with the results in Figure 4. For C_3 hydrocarbons, the production of allyl radicals (C_3H_5) reaches a maximum at 2500 K, which coincides with an increase in the production of propene and propyne. Figure 6 also shows that 1,3-butadiene is the primary C_4 intermediate observed during thermal decomposition, while the C_5 intermediates are dominated by 1,4-pentadiene, cyclopentene, and 1,4-pentadiene radical. At higher temperatures, we also observe the formation of acetylene and methane, which are not included in Figure 6 because their mole fractions are very small (<0.05 mol %). The high-temperature conditions used in these ReaxFF MD simulations preclude the formation of CPD, which is consistent with experimental observations.[5,8] Benzene, the other product observed experimentally, was proposed by Davidson et al.[9] to result from secondary chemistry, which would require times much longer than those in our current studies.

We used the rate of consumption of JP-10 as a guide to study the first-order kinetics of the pyrolysis. Figure 7 shows the consumption of JP-10 as a function of simulation time obtained from NVT-MD simulations at various temperatures ranging from 2000 to 2600 K. For each temperature, the number of JP-10 molecules consumed was averaged at each time point for 10 independent simulations. The rate constant at each temperature was determined from a linear fit to these data. From the Arrhenius plot in Figure 8, the activation energy (E_a) and pre-exponential factor (A) were determined to be 58.4 kcal/mol and 0.45×10^{14} s^{-1}, respectively. These Arrhenius parameters from the ReaxFF simulations are in good agreement with experimental values (E_a = 62.4 kcal/mol and $A = 57 \times 10^{14}$ s^{-1}).[12] In addition, the entropy of activation ($\Delta S^{\ddagger}$) was determined from ReaxFF to be 0.174 kcal K^{-1} mol^{-1} (729 J K^{-1} mol^{-1}), which

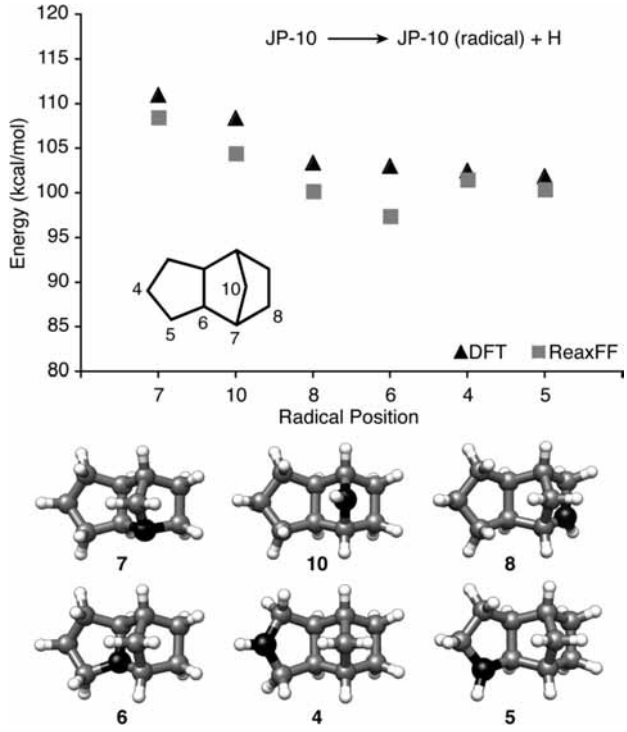

Figure 9. Comparison of the energies for the six unique homolytic C−H bond cleavages in the parent JP-10 molecule, as obtained from DFT and ReaxFF calculations for the corresponding JP-10 radicals. The radical position is designated by the carbon number and is colored black in the corresponding structure.[26]

is within 5% of the experimental $\Delta S^{\ddagger}$ value of 0.165 kcal K^{-1} mol^{-1} (692 J K^{-1} mol^{-1}).[12] This positive entropy is consistent with a transition state that is highly disordered compared with the ground state, as expected for a decomposition process. The activation energy obtained from the ReaxFF simulations can be attributed to a combination of C−C bond cleavage (for $H_3CH_2C-CH_2CH_3$, 86.8 kcal/mol[24]) and release of the strain in the JP-10 molecules (23.8 kcal/mol[3]), suggesting a barrier of 63 kcal/mol on the basis of experimental values only. The use of ReaxFF values for C−C bond cleavage in butane (78.8 kcal/mol) with the strain in JP-10 (23.2 kcal/mol) predicts an activation barrier of 55.6 kcal/mol. These predictions are consistent with the value of 58.4 kcal/mol calculated using ReaxFF simulations and the experimental value of 62.4 kcal/mol.

We analyzed hydrogen abstraction reactions that are likely to be important in the oxidation of hydrocarbons[19,25] by calculating the energy required to homolytically cleave a C−H bond in JP-10 to form hydrogen and JP-10 radicals. This allowed us to evaluate the stability of various JP-10 radicals. The QM and ReaxFF results are compared in Figure 9, where the geometry of each radical is also given.[26] The overall trend in the stabilities of JP-10 radicals obtained from ReaxFF is in good agreement with that from QM, validating the use of ReaxFF for studying the oxidation of this fuel. In addition, we found good agreement for the oxidation of various simple hydrocarbons, including methane, propene, *o*-xylene, and benzene, using the same ReaxFF force field, thereby providing an additional validation of the method.[19]

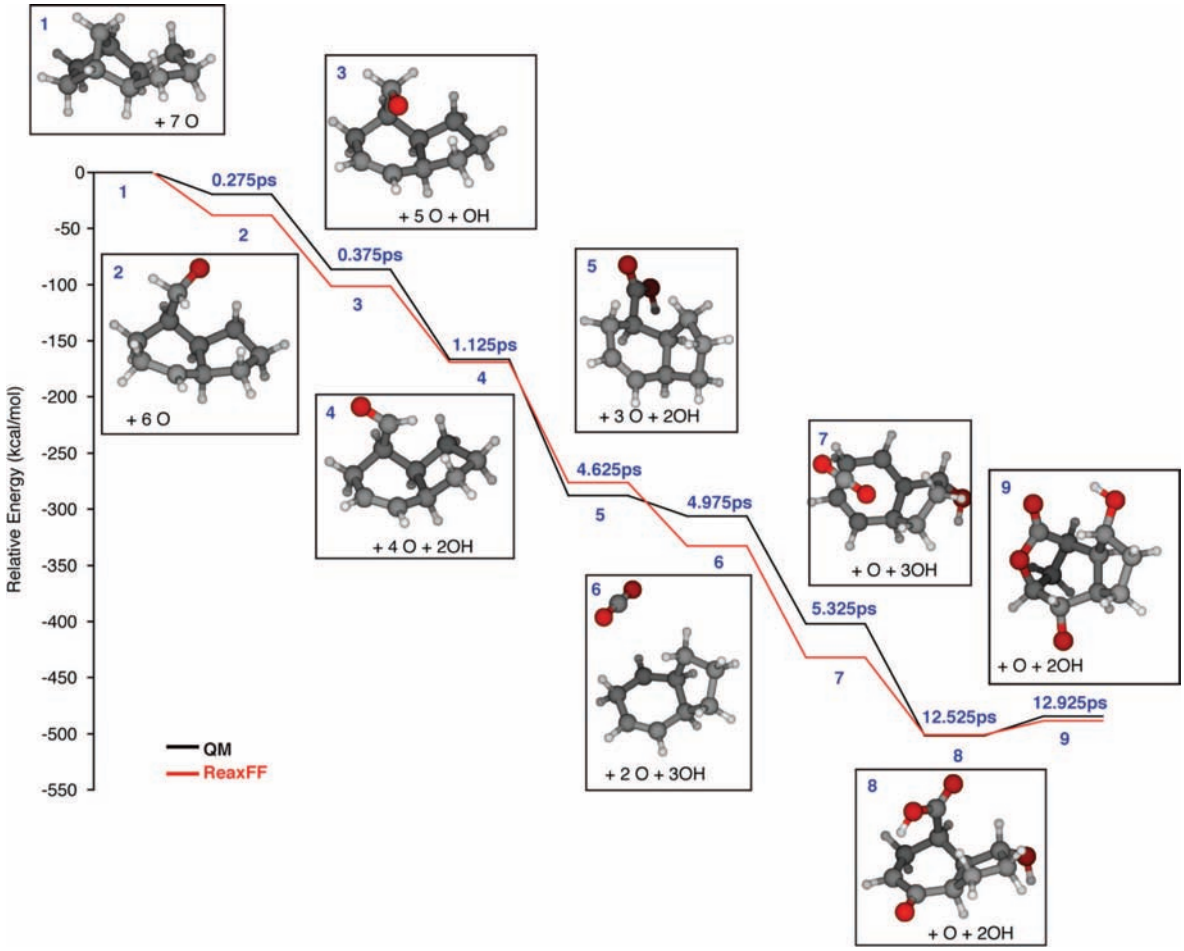

Figure 10. Comparison of ReaxFF (red) and QM (black) energies for various steps in the mechanism of JP-10 oxidation observed during a ReaxFF NVT-MD simulation at 1000 K.

We carried out NVT-MD simulations to test the ability of ReaxFF to elucidate the initiation mechanism for the oxidation of JP-10. Here the periodic cell contained five JP-10 molecules and 10 oxygen atoms. With oxygen radicals, we were able to observe rapid reactions at a temperature of 1000 K. The initial reaction (**1** → **2**, Figure 10) involves oxidation of the methylene carbon (carbon 10 in Figure 1), leading to scission of the C1−C10 bond. This is followed by a hydrogen abstraction reaction at carbon 9 by an additional oxygen radical, forming a double bond between C1 and C9 in the hydrocarbon intermediate (**2** → **3**, Figure 10). Subsequent hydrogen abstraction at C10 by an oxygen radical results in the aldehyde **4** and a hydroxyl radical, and this is followed by further oxidation of the aldehyde to carboxylic acid **5**. Intermediate **5** is converted to **6** via hydrogen abstraction and concomitant decarboxylation, resulting in the hydrocarbon intermediate and CO_2. Product **6** then undergoes hydroxylation at C5 followed by recombination with CO_2, leading to **8**. Next, oxidation at C1 followed by an intramolecular hydrogen transfer leads to **9**.

To validate the use of ReaxFF for these reactions, we also computed QM reaction energies for the reactions predicted by ReaxFF. Here we minimized the various intermediates taken from the ReaxFF MD trajectory. The QM and ReaxFF energies for the oxidation of JP-10 are compared in Figure 10, which shows that all of the reactions except **8** → **9** are exothermic. The overall thermodynamics obtained from QM is in excellent agreement with the ReaxFF description. Minimizing the ReaxFF intermediates led in some cases to coordination of a CO_2 species with the hydrocarbon intermediate, whereas the QM calculations found that these species were not bound. The bond energy for CO_2−**6** (Figure 10) using ReaxFF is 9.6 kcal/mol with a small barrier [∼12 kcal/mol using a low-temperature (25 K) constrained MD simulation to drive the coordination reaction], whereas CO_2 is not bound to **6** in the QM calculation. Probably the correct answer is somewhere in between.

This initial test of the ReaxFF force field for studying the oxidation of JP-10 validates the use of this method for investigating the combustion of hydrocarbon fuels.

Conclusions

We applied the ReaxFF force field for hydrocarbons to study the thermal decomposition and oxidation of JP-10. The ReaxFF NVT-MD simulations suggest that the thermal decomposition of JP-10 is initiated by C−C bond cleavage, resulting in either (1) production of ethylene plus a C_8 hydrocarbon or (2) two C_5 hydrocarbons, as found experimentally. We found the temperature dependence of the product distribution, particularly for C_1−C_5, to be in good agreement with experimental observations.

The rate of consumption of JP-10 as a function of temperature leads to an activation energy of 58.4 kcal/mol for JP-10 pyrolysis, which is consistent with experiment (62.4 kcal/mol) and with the effects of strain release upon cleavage of the C−C bond in the JP-10 molecule.

In addition, the ReaxFF NVT-MD simulations provide a reasonable reaction pathway for the oxidation of JP-10 that is thermodynamically consistent and has been validated against the results of QM calculations.

These results validate that ReaxFF can be used to obtain insight into the initiation mechanisms and product distributions associated with pyrolysis and oxidation processes for hydrocarbons.

Acknowledgment. This research was supported in part by ONR, ARO-MURI, and ONR-PROM. The computer systems were funded by ARO-DURIP and ONR-DURIP.

Supporting Information Available: ReaxFF force field parameters and a full description of the ReaxFF potential functions. This material is available free of charge via the Internet at http://pubs.acs.org.

References and Notes

(1) Li, S. C.; Varatharajan, B.; Williams, F. A. *AIAA J.* **2001**, *39*, 2351.

(2) (a) Knappe, B. M.; Edwards, C. F. In *Combustion Processes in Propulsion*; Roy, G. D., Ed.; Elsevier Butterworth-Heinemann: Boston, 2006; pp 273−282. (b) Dean, A. J. In *Proceedings of the 39th AIAA/ASME/SAE/ASEE Joint Propulsion Conference and Exhibit*, Huntsville, AL, July 20−23, 2003; AIAA 2003-4510. (c) Bussing, T.; Pappas, G. In *Proceedings of the 32nd Aerospace Sciences Meeting and Exhibit*, Reno, NV, January 10−13, 1994; AIAA 94-0263.

(3) Boyd, R. H.; Sanwal, S. N.; Shary-Tehrany, S.; McNally, D. *J. Phys. Chem.* **1971**, *75*, 1264.

(4) Davidson, D. F.; Horning, D. C.; Oehlschlaeger, M. A.; Hanson, R. K. In *Proceedings of the 37th AIAA/ASME/SAE/ASEE Joint Propulsion Conference and Exhibit*, Salt Lake City, UT, July 8−11, 2001; AIAA 01-3707.

(5) Van Devener, B.; Anderson, S. L. *Energy Fuels* **2006**, *20*, 1886.

(6) (a) Bruno, T. J.; Huber, M. L.; Laesecke, A.; Lemmon, E. W.; Perkins, R. A. *Thermochemical and Thermophysical Properties of JP-10*; NISTIR 6640; June 2006. (b) Steele, W. V.; Chirico, R. D.; Knipmeyer, S. E.; Smith, N. K. *High-Temperature Heat-Capacity Measurements and Critical Property Determinations Using a Differential Scanning Calorimeter: Results of Measurements on Toluene, Tetralin, and JP-10*; NIPER-395 (DE89000749); U.S. Department of Energy: Bartlesville, OK, June 1989.

(7) Herbinet, O.; Sirjean, B.; Bounaceur, R.; Fournet, R.; Battin-Leclerc, B.; Scacchi, G.; Marquaire, P. M. *J. Phys. Chem. A* **2006**, *110*, 11298.

(8) (a) Nakra, S.; Green, R. J.; Anderson, S. L. *Combust. Flame* **2006**, *144*, 662. (b) Green, R. J.; Nakra, S.; Anderson, S. L. In *Combustion Processes in Propulsion*; Roy, G. D., Ed.; Elsevier Butterworth-Heinemann: Boston, 2006; pp 355−364.

(9) Davidson, D. F.; Horning, D. C.; Herbon, J. T.; Hanson, R. K. *Proc. Combust. Inst.* **2000**, *28*, 1687.

(10) Cooper, M.; Shepherd, J. E. In *Proceedings of the 39th AIAA/ASME/SAE/ASEE Joint Propulsion Conference and Exhibit*, Huntsville, AL, July 20−23, 2003; AIAA 2003-4687.

(11) Wohlwend, K.; Maurice, L. Q.; Edwards, T. *J. Propul. Power* **2001**, *17*, 1258.

(12) Rao, R. N.; Kunzru, D. *J. Anal. Appl. Pyrolysis* **2006**, *76*, 154.

(13) Striebech, R. C.; Lawrence, J. *J. Anal. Appl. Pyrolysis* **2003**, *70*, 339.

(14) Galligan, C. Ph.D. Thesis, Universite Laval, Quebec, Canada, 2005.

(15) van Duin, A. C. T.; Dasgupta, S.; Lorant, F.; Goddard, W. A., III *J. Phys. Chem. A* **2001**, *105*, 9396.

(16) (a) Strachan, A.; van Duin, A. C. T.; Chakraborty, D.; Dasgupta, S.; Goddard, W. A., III *Phys. Rev. Lett.* **2003**, *91*, 098301. (b) Strachan, A.; Kober, E. M.; van Duin, A. C. T.; Oxgaard, J.; Goddard, W. A., III *J. Chem. Phys.* **2005**, *122*, 054502.

(17) van Duin, A. C. T.; Zeiri, Y.; Dubnikova, F.; Kosloff, R.; Goddard, W. A., III *J. Am. Chem. Soc.* **2005**, *127*, 11053.

(18) Chenoweth, K.; Cheung, S.; van Duin, A. C. T.; Goddard, W. A., III; Kober, E. M. *J. Am. Chem. Soc.* **2005**, *127*, 7192.

(19) Chenoweth, K.; van Duin, A. C. T.; Goddard, W. A., III *J. Phys. Chem. A* **2008**, *112*, 1040.

(20) Berendsen, H. J. C.; Postma, J. P. M.; van Gunsteren, W. F.; DiNola, A.; Haak, J. R. *J. Chem. Phys.* **1984**, *81*, 3684.

(21) Becke, A. D. *J. Chem. Phys.* **1993**, *98*, 5648. Lee, C.; Yang, W.; Parr, R. G. *Phys. Rev. B* **1998**, *37*, 785.

(22) Krishnan, R.; Binkley, J. S.; Seeger, R.; Pople, J. A. *J. Chem. Phys.* **1980**, *72*, 650.

(23) *Jaguar*, version 7.0; Schrödinger, LLC: Portland, OR, 2005.

(24) Luo, Y.-R. *Handbook of Bond Dissociation Energies in Organic Compounds*; CRC Press: New York, 2003.

(25) Simmie, J. M. *Prog. Energy Combust. Sci.* **2003**, *29*, 599.

(26) Structures were rendered using UCSF Chimera, Resource for Biocomputing, Visualization, and Informatics, at the University of California, San Francisco (supported by NIH P41 RR-01081). Pettersen, E. F.; Goddard, T. D.; Huang, C. C.; Couch, G. S.; Greenblatt, D. M.; Meng, E. C.; Ferrin, T. E. *J. Comput. Chem.* **2004**, *25*, 1605.

JP8081479